Antimicrobial organic–inorganic composite membranes including sepiolite-supported nanometals†

Berta Díez,[a] Javier Santiago-Morales,[a] María Jesús Martínez-Bueno,[b] Amadeo R. Fernández-Alba[b] and Roberto Rosal*[a]

In this study, composite polysulfone–polyvinylpyrrolidone (PSU–PVP) membranes were prepared using silver and copper loaded sepiolite as a filler. Metal-loaded sepiolite was evenly dispersed within the membranes. No leaching of metal particles was observed during use and only dissolved metals were responsible for membrane antimicrobial activity. The membranes displayed high antibacterial activity showing surfaces free of bacterial colonisation (<20 CFU cm^{-2}). *Escherichia coli* was inactivated at a higher rate (below detection limit in less than 60 min for silver sepiolite loaded membranes) than *Staphylococcus aureus*. All membranes could be successfully reused after daily inoculations and subsequent washing allowing up to 20 cycles with <99.999% CFU removal. The silver leached daily represented $\cong$0.2–0.4% of the total initial silver content of membranes (0.8–1.0% for copper in copper-containing membranes). Despite its initial lower rate of inactivation, the resistance to *S. aureus* colonisation lasted longer than that to *E. coli* in an assay consisting of daily inoculations on the same membranes.

Introduction

The demand for new water resources has become increasingly urgent worldwide due to a fast growing global population and an increasing water demand. Global warming is expected to lead to a severe decrease in freshwater resources even doubling the effect of population growth alone.[1] Membranes play a central role in water and wastewater treatment with continuous technology improvements, new uses and cost reductions.[2] Ultrafiltration is the established technology for reclaiming wastewater and for the pre-treatment of seawater prior to reverse osmosis, the two major processes aiming to expand water resources.[3,4] Polysulfone and polyethersulfone are the most common materials for preparing ultrafiltration membranes due to their good mechanical and chemical properties, easy processing and wide availability.[5] However, a major problem of polysulfone or polyethersulfone membranes is that their hydrophobic nature favours a relatively rapid loss of permeate flow due to fouling and biofouling, which are the main factors determining membrane performance in practical

applications.[6] Fouling is a consequence of the adsorption and deposition of solutes, while biofouling refers to the growth of microorganisms on membrane surface. Both cause loss of permeability, increased transmembrane pressure and shorten membrane life. The formation of biofilm layers also supposes a serious risk of pathogen proliferation.[7] Several strategies have been developed for controlling membrane biofouling in order to prevent or reduce bacterial attachment. They include disinfection using biocidal treatments, nutrient limitation and the modification of the physicochemical properties of membranes.[8] Membrane materials, particularly membrane surface, can be modified in order to render membranes with improved resistance to bacterial attachment. For example, modifying hydrophobicity and roughness, which have been associated to higher biofouling potential due to stronger membrane–bacteria interactions.[9] The increase of membrane hydrophilicity has been widely explored with the added value that it is an approach also valid for mitigating non-biological fouling and to increase membrane permeability.[10] Surface modifications and the use of additives have been reported by several researchers in order to prepare hydrophilic membranes.[11–12] A commonly additive used for this purpose is polyvinylpyrrolidone (PVP).[13,14] Besides being highly hydrophilic, PVP reduces the miscibility of casting solutions with non-solvent water, which enhances phase separation during membrane fabrication.[15]

Another approach is to provide antimicrobial properties by loading materials able to inhibit microbial growth. The use of metal-loaded antimicrobial materials exploits the well-known oligodynamic action of some metals, notably silver and

[a]Department of Chemical Engineering, University of Alcalá, 28871 Alcalá de Henares, Madrid, Spain. E-mail: roberto.rosal@uah.es

[b]Department of Analytical Chemistry, University of Almería, European Union Reference Laboratory for Pesticide Residues in Fruit & Vegetables, Agrifood Campus of International Excellence (ceiA3), E-04010, Almería, Spain

† Electronic supplementary information (ESI) available: The composition of casting solutions, TEM micrographs of sepiolites, SEM-EDS micrographs of membranes, membrane properties, ATR-FTIR and XRD spectra as well as rate constants for microbial inactivation are presented. See DOI: 10.1039/c6ra26044f

copper, which strongly inhibit microbial growth.[16,17] Accordingly, silver and copper-loaded membranes have been used to prevent bacterial attachment and reduce biofilm formation.[18,19] The mechanism of action of metals in their nanoforms has been debated in the scientific literature, particularly for the case of silver.[20] The discussion tried to determine whether the release of ion metals is the only reason for their antimicrobial action or nano-bio interactions play a significant role. It has been recently shown that silver nanoparticles exert a biological effect only in aerobic conditions, which are the only that make it possible the release of silver ions, which suggests that specific nanoparticle interactions are probably not relevant.[21] The advantage of using metals in nanoparticle form would be to exploit their role as nanocarriers based on the higher rate of dissolution of particles with large surface area. However, nanoforms must tackle the problem of their possible release into the environment, which is a major concern in view of the potential risk of nanoparticles.[22] The attachment of nanometals to supports, rather than the direct dispersion of nanoparticles into the polymeric solution, is a possibility to overcome this problem by making migration more difficult or impossible.[23]

The objective of this study was to prepare composite polysulfone ultrafiltration composite membranes including a source of silver and copper ions using sepiolite fibers as metal reservoir. Sepiolite acts as a vehicle for introducing silver nanoforms and copper salts into the polymeric solution avoiding the problems derived from nanoparticle aggregation or chemical incompatibility with casting solvents. Moreover, the fact that the metals were attached to a silicate was expected to impart stability and minimize the risk of nanoparticle dissemination into the environment. Membranes were produced using a conventional phase inversion process and were tested using strains of the Gram-negative bacterium *Escherichia coli* and the Gram-positive *Staphylococcus aureus*. Special attention has been paid to assess the release of metal nanoparticles and membrane durability.

Experimental

Materials

Polysulfone (PSU, 60 kDa) and 1-methyl-2-pyrrolidone (NMP) were purchased from Acros Organic. Polyvinylpyrrolidone (PVP, 40 kDa) was obtained from Sigma-Aldrich. The components of culture media were biological grade acquired from Conda-Pronadisa (Spain). Ultrapure water was generated from a Direct-Q™ 5 Ultrapure Water Systems from Millipore (Bedford, MA, USA) with a specific resistance of 18.2 MΩ cm.

Sepiolite is a porous hydrated magnesium silicate with a large specific surface area and a needle-like morphology with high surface area and exceptional sorptive properties. Silver, copper and silver/copper-loaded sepiolites were produced by Tolsa S.A, Spain using a procedure described elsewhere.[24] Briefly, a mechanically dispersed sepiolite was put in contact with the precursor salts at low pH in order to favour magnesium lixiviation and the introduction of metallic cations. The addition of NaOH induced the precipitation of silver hydroxide or hydrated copper nitrate. The materials were then washed and dried at

a minimum temperature of 150 °C yielding nanoparticles of silver and a mixture of copper compounds depending on the drying conditions. In this case copper-containing sepiolite was not reduced and, therefore, copper was not forming metallic nanoparticles, but amorphous copper hydroxide, with minor contribution of copper oxide. As a result of the thermal treatment, sepiolite channel structure collapsed and nanoparticles got embedded into the silicate structure as well as attached to their surface. The advantage of this process is that the metals or metal compounds became supported on particles with a non-nano dimension, which makes them easier to handle and limits the risk of their release into the environment. It also allows a high weight load of active metals. The explanation on how sepiolite can be used as a host for different metallic cations upon magnesium leaching and the material acting as scaffold for the growth of metal nanoparticles can be found elsewhere.[25]

Sepiolite composition was determined by ICP-MS using a NexION 300XX Perkin-Elmer apparatus after microwave digestion according to the prescriptions of EPA Method 3052 in a Mileston Ultra-WAVE equipment. Silica and magnesium were also determined by ICP-MS, which allowed to close the balance with a global error <5%. The composition of the three sepiolites used was, expressed as metal, 17.6 ± 0.5 wt% Ag for silver–sepiolite (SpAg), 12.8 ± 0.8 wt% Cu for copper–sepiolite (SpCu) and 7.9 ± 0.4 wt% Ag and 9.5 ± 0.7 wt% Cu for the mixed silver/copper–sepiolite (SpAgCu). Fig. S1 (ESI†) shows TEM images of sepiolite loaded with silver, silver–copper and copper. Silver nanoparticles displayed a relatively broad nanoparticle size distribution, approximately ranging from 5–50 nm, enclosed or supported on the sepiolite fibrillar structure. It is important to note that copper hydroxide was not visible in TEM images and only silver nanoparticles do as black dots. Sepiolite fibers had an average length of 1–2 μm, and ~20 nm width.

Membrane preparation

Control PS and composite membranes with metal-loaded sepiolite were prepared *via* phase inversion. The casting solution was prepared by dissolving PVP in NMP followed by stirring until suspension. The required amount of metal-loaded sepiolite was added to the aforementioned solution and dispersed in an ice-water bath. Control materials were also prepared without PVP. PSU was then added and the mixture magnetically stirred for another 2 h at 70 °C. Table 1 shows the chemical composition of casting solutions and the nomenclature used in what follows.

The casting solution was degassed for 10 min and casted on the glass plate of an automatic film applicator AB3120 (TQC, The Netherlands) adjusted to a thickness of 200 μm. Immediately after, the membrane was immersed into a distilled water bath at 16 °C for 1 min. After the immersion, the membrane was removed and its surface was cleaned with water and kept in distilled water for 24 h to remove residual solvent. Prior to storage, the membranes were dried at 50 °C and then vacuum-dried at 90 °C (−0.9 bar) during 24 h. Some membranes were irradiated with ultraviolet (UV) radiation at room temperature for using a Vilber-Lourmat Bio-Lin BLX-254 Crosslinker equipped with 5×8 W 254 nm T-8C lamps. The irradiance was 820 μW cm^{-2}.

Table 1 Composition of casting solutions[a]

Membrane	Identifier	PSU (wt%)	PVP (wt%)	NMP (wt%)	Filler (wt%)
PSU (control)	M(0)	15.0	—	85.0	—
SpAg-1@PSU	M(1)	15.0	—	84.9	0.15
SpAg-5@PSU	M(2)	14.9	—	84.3	0.78
PSU–PVP-5	M(3)	15.0	0.79	84.2	
PSU–PVP-10	M(4)	15.0	1.67	83.3	
PSU–PVP-15	M(5)	15.0	2.65	82.3	
PSU–PVP-25	M(6)	15.0	5.01	80.0	
SpAg@PSU–PVP-5	M(7)	14.9	0.78	83.4	0.99
SpAg@PSU–PVP-10	M(8)	14.9	1.65	82.5	0.99
SpAg@PSU–PVP-15	M(9)	14.9	2.62	81.5	0.99
SpAg@PSU–PVP-25	M(10)	14.9	4.96	79.2	0.99
SpAgCu@PSU–PVP-5	M(11)	14.9	0.78	83.4	0.99
SpCu@PSU–PVP-5	M(12)	14.9	0.78	83.4	0.99

[a] PSU–PVP-x means x wt% PVP with respect to the total amount of PSU + PVP. The filler was sepiolite and represented 1 and 5 wt% respectively in SpAg-1@PSU and SpAg-5@PSU specimens. For the rest of sepiolite-loaded materials, the amount of sepiolite was ~5 wt%.

Membrane characterization

The morphology of membrane cross-section was observed using Scanning Electron Microscopy (SEM) in a XL-30 Philips apparatus. Surface porosity was observed using a Field Emission Scanning Electron Microscope (FE-SEM) in a Hitachi SU8000 equipment operating at 1 kV on non-metalized samples coated with graphite (Fig. S2†). Elemental analyses of the membranes were carried out using SEM combined with energy dispersive X-ray spectroscopy (EDS) JEOL JSM 6400 operating at an acceleration voltage of 20 kV (Fig. S3†). SEM images of membranes exposed to bacterial colonisation were obtained in a ZEISS DSM-950 instrument operating at 25 kV. For it, clean membranes were inoculated with 0.15 mL mg^{-1} of nutrient broth (NB), pH 7.0 ± 0.1 with 10^6 cells per mL and incubated for 20 h at 36 °C, after which membranes were cleaned with phosphate buffered saline (PBS), fixed and dehydrated with ethanol and acetone prior to SEM imaging.

The hydrophilicity of membranes was determined by measuring water contact angles of vacuum-dried specimens (90 °C, 2 hours). Each measurement was conducted in triplicate using the sessile drop technique using an optical contact angle meter (Krüss DSA25 Drop Shape Analysis System) operating at room temperature. Surface ζ-potential was measured via electrophoretic light scattering (DLS, Malvern Zetasizer Nano ZS) and using a Surface Zeta Potential Cell (ZEN 1020) from Malvern. A rectangular section of the membrane was taped on the sample holder using Araldite adhesive. The cell was inserted into a disposable 10 mm square cuvette containing 10 mM KCl, pH 7.0, aqueous solution with of 0.5% (w/w) polyacrylic acid (450 kDa) used as a tracer (a negatively-charged tracer is required for negatively-charged surfaces). Measurements were conducted at 25 °C at six different displacements from the sample surface in order to calculate the surface ζ-potential. Fig. S4† shows ζ-potential for all tested specimens.

Attenuated total reflectance Fourier transform infrared (ATR-FTIR) spectra were recorded using a Thermo-Scientific Nicolet iS10 apparatus with a Smart iTR-Diamond ATR module. ATR-FTIR spectra of the PSU and PSU–PVP-5 membranes before and after UV irradiation are shown in Fig. S5.† XRD spectra of PSU–PVP-5 membranes, metal loaded sepiolites and the composite membranes were recorded using an X-ray diffractometer PolycrystalX'pert Pro PANalytical which employed Ni-filtered Cu Kα ($k = 1.5406$ nm) radiation and operated at 0.02 min^{-1}, 45 kV and 40 mA (Fig. S6).†

Membrane filtration studies

Membrane permeability was measured in a Millipore filtration cell with an effective membrane area of 28.7 cm^2 and a total cell volume of 100 mL using membranes preconditioned in distilled water. Membrane permeability was determined from the pure water flux, J, per unit transmembrane pressure (TMP):

$$P = \frac{J}{\Delta P} \tag{1}$$

The average surface pore radius of the membranes, r_m, was estimated using the filtration velocity method according to the Guerout–Elford–Ferry equation:

$$r_m = \sqrt{\frac{(2.9 - 1.7\varepsilon)8JL\eta}{\varepsilon \Delta P}} \tag{2}$$

The mean radius obtained is considered a cross-sectional average of all the pores involved in permeate flow. η is the water viscosity: 8.9×10^{-4} Pa s. Membrane porosity, ε, was determined by water uptake using the weights of wet and dry membranes. All measurements were performed in triplicate using a TMP pressure difference of 0.20 MPa at 20 °C.

Metal and nanoparticle release studies

ICP-MS analyses of metal released from membranes were performed on an ICP-MS model X Series 2 system apparatus from Thermo Scientific. The calibration curve was prepared by using standards in ultrapure water 1% HNO$_3$ (v/v). Dynamic and static

tests for metal release were carried out in order to assess the rate of liberation/migration of active metals from membranes.

In static tests, membranes were submerged in ultrapure water with or without 150 mg L^{-1} of NaCl, which was based on the parametric values established for chloride (250 mg L^{-1}) and sodium (200 mg L^{-1}) by the European Drinking Water Directive, Council Directive 98/83/EC, for water intended for human consumption. The experiments were performed at 20 °C using 50 mL of water in opaque glass bottles for a contact time of up to 4 days in static runs.

In order to quantify the release of metals under flow conditions and to assess the possible release of nanoforms during membrane use, a dynamic experiment was performed that consisted of taking samples at different cumulative volumes representing a total filtration time of approx. 6 h. The samples were further ultrafiltrated using Vivaspin 20, 5 kDa, polyethersulfone ultrafiltration centrifuge tubes. A 5 kDa membrane would retain particles over 2 nm, larger than the smaller silver nanoparticles found attached to sepiolite.[26] The samples were then analysed for metals using ICP-MS. In case of nanoparticle release, the amount detected in the 5 kDa ultrafiltrate would be significantly lower than that coming directly from membrane permeate. TMP was set at 2 bar and at least two replicates of each assay were performed.

Antimicrobial bioassays

The bioassays were performed using two bacteria, *E. coli* (CETC 516) and *S. aureus* (CETC 240), which are the strains suggested by the ISO 22196† concerning the measurement of antibacterial activity on plastic surfaces. The bacteria were preserved at −80 °C in glycerol (20% v/v) until use. Reactivation was performed by culture in nutrient broth (10 g L^{-1} peptone, 5 g L^{-1} sodium chloride, 5 g L^{-1} meat extract and, in case of solid medium, 15 g L^{-1} powder agar). pH was adjusted to 7.0 ± 0.1 using NaOH or HCl. Bacterial growth was measured by optical density (OD) at 600 nm.

The membranes to be tested for antimicrobial behaviour were placed in sterile 24 well microplates and exposed to cultures containing an initial concentration of 10^6 cells per mL. The volume of test inoculum was fixed at 0.15 mL mg^{-1} of membrane. Incubation took place at 36 °C during 20 h. After incubation, the viable bacteria were measured both in cultures in contact with membranes and on membrane surface. For cultures, 10-fold serial dilutions were performed in phosphate-buffered physiological saline (PBS) and 10 μL of the dilution was spot-plated on solid agar and incubated at 36 °C for 24 h, after which, the number of colonies were counted. The number of viable bacteria on membrane surface was determined after detaching them by means of the following procedure. First, the membranes kept in contact with microorganisms were recovered and transferred to sterile 24-well microplates and washed with PBS for 25 min in an orbital shaker. Then, PBS was replaced with 2 mL of SCDLP broth (soybean casein digest broth with lecithin and polysorbate according to ISO 22196) in order to remove bacteria from membrane. Microplates were kept under mechanical agitation for 30 min. SCDLP liquid was

serially diluted in PBS and 10 μL of each dilution was spot-plated on agar. All samples were measured in triplicate.

The durability of the antimicrobial effect of membranes with metal-loaded sepiolites was assessed by performing successive inoculation of *E. coli* or *S. aureus* on the same membrane specimens after removing the preceding culture by careful washing. The membranes were placed in 24-well microplates and exposed to 10^6 cells per mL (0.15 mL mg^{-1} of membrane) using a 500-fold diluted nutrient broth (1/500 NB) at 36 °C for 20 h. After the prescribed time, samples from the culture in contact with membranes were serially diluted in order to count viable bacteria according to the procedure described before. The minimum number of colonies assessed was 10 CFU mL^{-1}. The used membranes were transferred to new sterile wells and incubated with the same inoculum (10^6 cells per mL in 1/500 NB). The same procedure was repeated as many times as required until bacterial colonies appeared in the liquid. The number of cycles of inoculation and washing without microbial growth was considered an indicator of the service life of membranes. Finally, the biocidal activity of metal-loaded membranes was evaluated from the rate of decay of viable cells during the period immediately after inoculation with 10^6 cells per mL in 1/500 NB. Supernatant broth was sampled at different times and viable bacteria were counted as described before.

Results and discussion

Membrane properties and performance

The surface morphology of membranes is shown in Fig. S2† for three representative specimens. Sepiolite loaded and non-loaded membranes exhibited a porous surface with a relatively thin skin layer and internal sponge-wall asymmetric morphology showing large, finger-like macrovoids. PSU–PVP and composite specimens did not display any significant evident differences in macrovoid structure or skin layer thickness. This result was in agreement with the porosity measurements shown in Fig. S4,† which reveals a trend towards higher porosity for membranes containing sepiolite materials, M(7) to M(10) compared to PSU–PVP. The increase of membrane porosity with hydrophilic fillers is a well-known fact explained as a consequence of the faster interdiffusion process resulting from their addition to the ternary thermodynamic system.[27]

Fig. 1 shows membrane permeability and pore sizes calculated from eqn (1) and (2). Our results showed that the introduction of PVP resulted in larger water permeability and increased surface pore sizes but the differences were only clearly observed for membranes with up to 10 wt% PVP. The use of the non-solvent hydrophilic additive PVP, reduces the miscibility of casting solutions with water and has been shown to enhance phase separation up to a certain concentration. Accelerating demixing contributes to the enlargement of membrane surface pores with a parallel increase in permeability.[28] The results agreed with previous findings and showed a trade-off between thermodynamic and kinetic factors controlling the demixing process during phase separation. The permeability increases with PVP concentration due to the enhanced phase separation
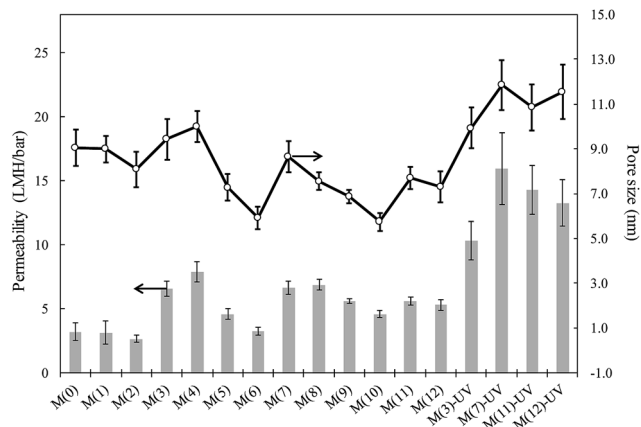
Fig. 1 Water permeability (bars, left scale) and surface pore sizes calculated according to the Guerout–Elford–Ferry equation (lines and circles, right scale).

but drops for higher concentrations due to the delayed demixing and the kinetic hindrance derived from the viscosity increase of the casting solution.[15,29] The introduction of sepiolite particles did not significantly alter water permeability or surface pore size with similar values for the SpAg@PSU–PVP membranes, M(7)–M(10), with respect to their counterparts without sepiolite, M(3)–M(6). Pore sizes were quite similar in all cases and always in the 5–12 nm range.

UV irradiated membranes displayed higher permeabilities than non-irradiated specimens. The functionalization of PSU membranes using techniques such as irradiation, plasma treatment or chemical agents is a well-known way of increasing the hydrophilicity of PSU membranes and, consequently, to increase membrane flux without using chemical additives.[30,31] The formation of carboxylic and sulfonic acid groups on membranes is supposed to create internal repulsion forces within the pores, which causes their enlargement and, therefore, an increase in permeability. We obtained surface ζ-potential values slightly less negative for composite membranes with respect to the neat PSU membrane (-53.9 ± 3.2 mV). The results are shown in Fig. S4† and could be attributed to the relatively lower negative charge of sepiolite particles, the ζ-potential of which was, at pH 7.0, -38.8 ± 7.2 for SpAg, -37.6 ± 5.2 mV for SpAgCu and -28.1 ± 4.8 mV for SpCu (measured in 10 mM KCl). The small difference in surface change for composite membranes including sepiolite particles suggests that the particles became completely entrapped into the polymeric matrix. Water contact angle measurements also support this assumption. PSU membranes were hydrophobic according to their water contact angle, which was 81° (± 3). The introduction of the hydrophilic PVP only slightly reduced contact angles, with a value of 73° (± 2) for 5 wt% PVP membranes. The addition of metal-loaded sepiolite did not significantly change surface hydrophilicity, but irradiated membranes were clearly more hydrophilic with an average contact angle of 43° ($\pm 2°$) for the irradiated specimens.

The changes in membrane surface were tracked by ATR-FTIR as shown in Fig. S5.† ATR-FTIR measurements on PSU and PSU–

PVP specimens gave information on chemical changes on membrane surface. The addition of PVP to PSU membrane led to a new band at 1674 cm^{-1}, which corresponds to amide I carbonyl peak.[32] PSU irradiated membranes show a new broad band around 1721 cm^{-1} linked to C=O stretching, which can be attributed to carboxyl groups and is compatible with the oxidative photolysis of aromatic groups from the outer membrane layer.[33] The band was clearly observed for PSU–UV membranes in which the PVP signal at 1674 cm^{-1} was absent. This was confirmed by a decrease in peaks at 1323 and 1236 cm^{-1} corresponding to sulfone and ether stretching respectively. It can also be observed that amide I peak shifted to 1666 cm^{-1}, what could correspond to formation of hydrogen bonds between carbonyl and hydroxyl groups from oxidized species of PVP or PSU.[34]

The presence of metals in membrane samples has been assessed by means of SEM-EDS (Fig. S2†), which shows the presence of silver and copper in composite membranes. It is interesting to note that the corresponding to metal appear frequently aligned in a row, corresponding to the direction of sepiolite fibers. (This alignment was highlighted in the inset of Fig. S2-A.†) The images show a good dispersion within membrane specimens without visible particle aggregation. The XRD spectra of PSU–PVP-5 membranes, metal loaded sepiolites and the composite membranes are shown in Fig. S6.† Silver loaded materials (SpAg and SpAgCu) show the typical XRD patterns of metallic silver with four sharp diffraction peaks at 2θ values of 38.0, 44.1, 64.3 and 77.3°, which corresponded to Bragg's reflections from the (111), (200) (220) and (311) planes of Ag and in good agreement with the reported data.[35] We got no peaks corresponding the cubic structure of silver oxide indicating that all the silver was in reduced form.[36] XRD of copper sepiolite shows less peaks, probably because of the amorphous nature of copper hydroxide. The small peaks appearing could be attributed to the (−111) and (111) planes of monoclinic copper oxide at 2θ 35.7 and 39.0°, although a precise assignment is difficult.[37]

Metal release and nanomaterial stability

The two reasons for using sepiolite as metal support were to ensure a good dispersion of nanoparticles in the polymeric solution and to avoid their release into the environment. In order to assess the possible migration of nanometals, a series of successive filtration runs were performed using the same membranes, the filtrates being analysed by ICP-MS before and after 5 kDa ultrafiltration. The results are shown in Fig. 2. The upper limit of the bars is the amount of silver or copper in the permeate of composite membranes, whereas the lower correspond to the same values in the 5 kDa ultrafiltrate of an aliquot of the first permeate. Significant differences between the upper and lower bar boundaries were only found for silver during the first batch, indicating that no nanoparticles were released except for silver during the first filtration period. These nanoparticles probably corresponded to the less tightly bound in the more accessible sepiolite fibers. Afterwards, the results showed that silver and copper could not migrate in nanoparticle form to the filtrate. A further evidence supporting this claim is that no
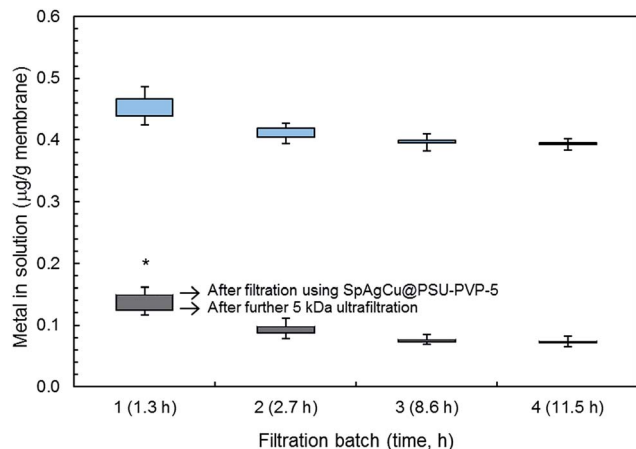
Fig. 2 ICP-MS analyses of silver (below, grey) and copper (upper, blue) measured in successive filtrations using SpAgCu@PSU–PVP-5 membranes and 5 kDa ultrafiltration of membrane permeate. Significant differences between the upper and lower limits were only found for silver in the first batch (asterisk). (Only the upper and lower parts of error bars are shown for clarity.)

significant amounts of silicon were found in ICP-MS analyses beyond the solubility limit of sepiolite itself, showing that sepiolite fibers did not detach from the polymer.

The same experiment combining filtration-ultrafiltration was performed with metal-loaded sepiolite materials kept in water suspension for one hour. ICP-MS analyses showing the amount of metals passing to the solution yielded 4.3 ± 0.3 µg g^{-1} of sepiolite for silver and 17.8 ± 1.5 µg g^{-1} of sepiolite for copper, which, considering the concentration of sepiolite filler in membranes (5 wt%) are figures comparable to those shown in Fig. 2. The amount of nanomaterials detached from sepiolite fibers (retained for 5 kDa UF) were 1.7 ± 0.5 µg g^{-1} of sepiolite for silver and 2.2 ± 0.6 µg g^{-1} of sepiolite for copper somewhat higher (after correcting for the 5 wt% concentration in membranes) than the values obtained for sepiolite loaded membranes most probably due to the stabilizing role of polymer for the less tightly attached metal particles.

Fig. 3 shows the amounts of copper and silver released by different membranes containing SpAg, SpAgCu and SpCu, (SpAg@PSU–PVP-5, SpAgCu@PSU–PVP-5 and SpCu@PSU–PVP-5) indicated as M(7), M(11) and M(12) respectively. Membrane specimens were kept for 4 days in water (and in water containing 150 mg L^{-1} NaCl). M(7) released more silver than M(11) as expected from its higher silver content. The percentage of silver leached could be estimated in both cases as approx. $\cong 0.2$–0.4% of their total initial silver content for every 24 h period (0.8–1.0% for copper in copper-containing membranes). Using these figures, a rough estimation of the time on service for membranes is provided below.

Metal release was higher for UV-irradiated membranes, probably due to their higher surface hydrophilicity, which would favour the access of water molecules and the migration of solvated cations (Ag^+, Cu^{2+}) or the hydroxylated species that dominate the speciation of copper, $Cu_2(OH)_2^{2+}$ and $Cu_3(OH)_4^{2+}$ according to visual MINTEQ (version 3.1, KTH, Stockholm,
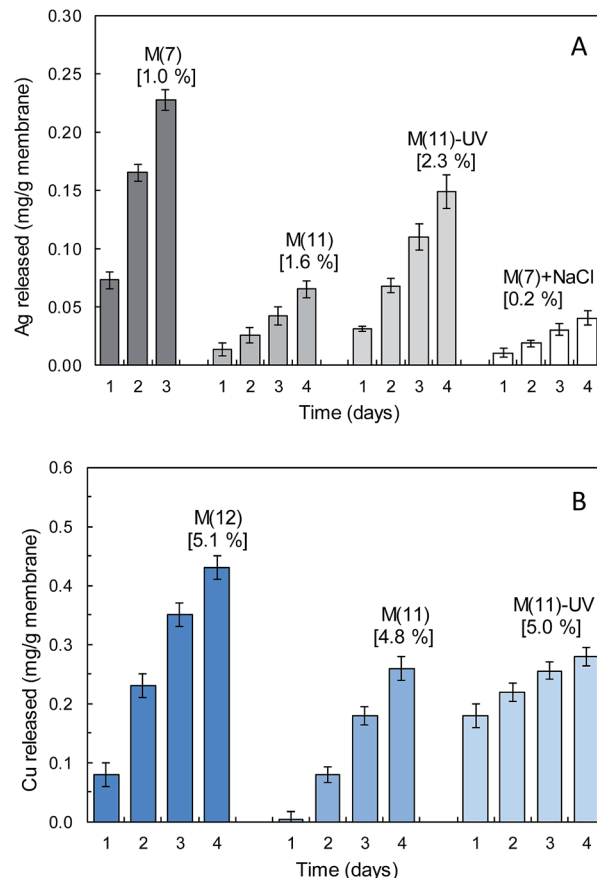

Fig. 3 Silver (A) and copper (B) released from M(7) (SpAg@PSU–PVP-5), M(11) (SpAgCu@PSU–PVP-5), M(12) (SpCu@PSU–PVP-5), M(11)-UV irradiated and M(7) + NaCl 150 mg L^{-1} membranes. Values in brackets show the percentage of metal with respect to the total metal content.

Sweden). In the presence of chloride, the amount of silver released was considerably lower due to the formation of insoluble AgCl (according to visual MINTEQ 150 mg L^{-1} NaCl yielded saturated solutions of AgCl for >50 µg Ag^+ per L and in all cases the concentration of AgCl(aq) was one order of magnitude higher than that of the free ion Ag^+). For copper, the results run in parallel, with higher metal release in irradiated membranes or in membranes with higher copper content (SpCu@PSU–PVP-5). The rate of release of copper was higher than that of silver because copper was already in the Cu(II) oxidation state in the sepiolite material, whereas silver required an additional oxidation step from Ag(0) to Ag^+. We preferred this material over sepiolite with Cu(0) or CuO because the amount of copper required for a biocidal effect is larger than that of silver due to its role as essential metal.[38]

It is interesting to note that the rate of release was essentially linear with time, which could be attributed to the difficulty of ions to dissolve and migrate from their nanoparticle support to the bulk. In a previous work, we obtained nanosilver composites with unsupported silver by taking advantage of the reducing effect of PVP. The result was a polymer loaded with silver nanoparticles in the tens of nanometre range. This procedure, however, leads to a rapid leaching of metals during the first

hours on stream accompanied by significant nanoparticle detachment.[39] The data presented here show no nanoparticle loss with only a certain preferential release of the more accessible metals on the surface of sepiolite.[23]

Antibacterial performance

Fig. 4 shows the result of microbial growth tests performed on different membrane specimens. Fig. 4(A) refers to the liquid in contact with membranes after incubation for 20 h at 36 °C, while the results for bacteria detached from surface (expressed as CFU per unit membrane surface) are shown in Fig. 4(B). The growth of *E. coli* and *S. aureus* was high for cultures in contact with PSU, not significantly lower than the 1/500 NB control without membrane. The addition of PVP led to membranes somewhat less prone to microbial adhesion, probably due to their more hydrophilic surface.[40,41] Other factors, however are involved such as surface charge, which is more negative for membranes with high PVP content, and may explain the higher amount of bacteria attached to M(6) in comparison with M(3) as shown in Fig. 4(B).

Upon contact with metal-loaded membranes the microbial growth was completely inhibited. The effect was considerable for M(2), a membrane prepared without PVP, but was much

more marked for composite membranes using PSU–PVP blends, M(7) to M(12). In this case, always for a total content of 5 wt% of metal-loaded sepiolite, microbial growth did not take place at all, and the combination of PSU–PVP and SpAg, SpAgCu and SpCu led to membranes free of any significant microbial growth after 20 h following inoculation. For the sake of clarity, Fig. 4 shows together the results for M(7) to M(10) (SpAg@PSU–PVP-5/10/15/25). All metal loaded membranes were free of bacteria with less than 20 CFU cm^{-2}.

Fig. 5 shows SEM micrographs of the surface of membranes put in contact with cultures of *E. coli* and *S. aureus* for 20 h at 36 °C (inoculum 10^6 cells per mL in 1/500 NB, washed, fixed and dried before imaging). The surface of PS–PVP-5 membranes appeared almost entirely colonized with bacteria, while SpAg@PSU–PVP-5 was clean except for a few cells and objects that are probably cell debris.

The antimicrobial effect of materials containing silver and copper nanoparticles is still controversial, with different pathways suggested for bacterial growth inhibition. In certain cases, nanoparticles can be internalized *via* phagocytosis and endocytosis, but sepiolite-loaded nanometals were not significantly released during membrane use as shown in Fig. 2. The increase in reactive oxygen species because of the interaction with the nanoparticle surface has been suggested to a least partly explain nanotoxicity.[42–45] Other studies suggested that the mechanism of silver nanoparticle toxicity would be essentially explained by the release of silver ions due to the reaction with dissolved oxygen.[46] In our case, membrane surface properties, the good metal dispersion shown by SEM-EDS micrographs and the absence of nanoparticle release from composite membranes suggest that the sepiolite material is well dispersed and entangled into the polymer matrix. Consequently, the amount
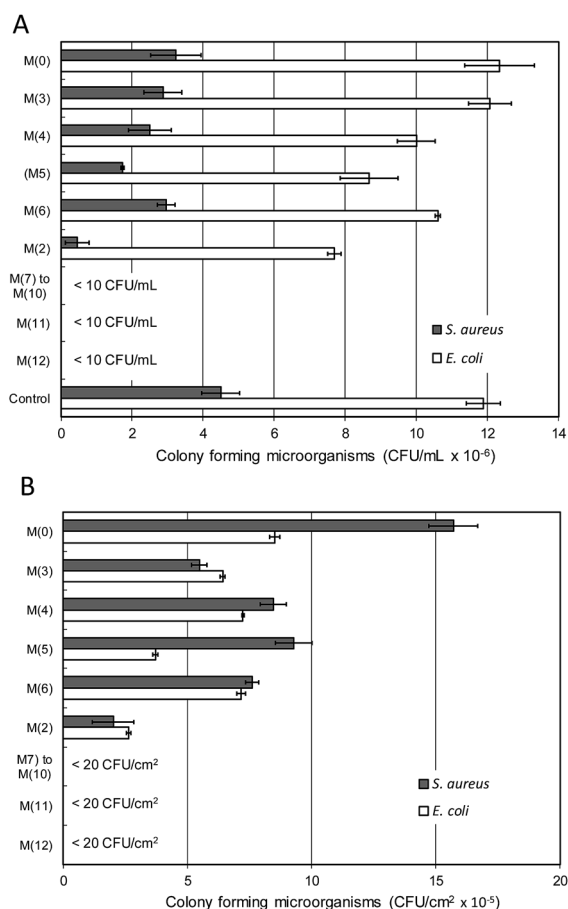

Fig. 4 Microbial growth for bacterial cultures exposed to different membranes (A) and culturable bacteria detached from membranes after incubation (B) at 36 °C, 20 h.
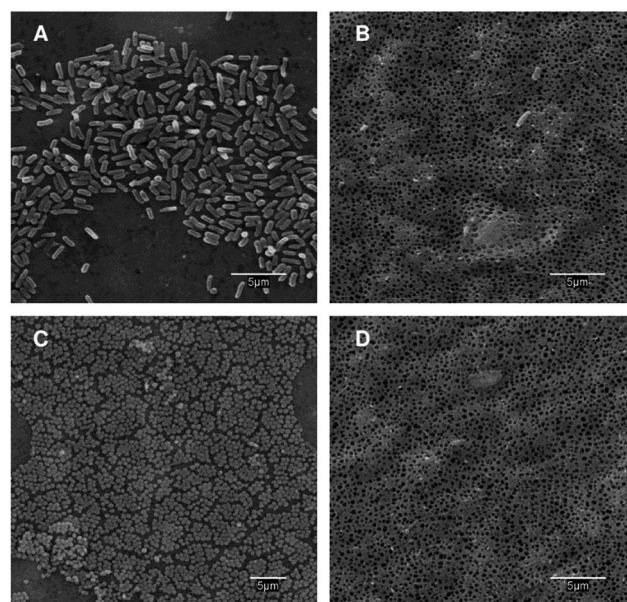

Fig. 5 SEM micrographs of PS–PVP-5 (A and C) and SpAg@PSU–PVP-5 (B and D) membranes cultured for 20 h at 36 °C and pH 7.0 with an initial inoculum of 10^6 cells per mL (0.15 mL mg^{-1} membrane) of *E. coli* (A and B) and *S. aureus* (C and D).

of nanoparticles in the skin layer that could get in touch with bacterial cells, would be limited if any. Also supporting this claim is that surface charge was similar for all membrane specimens. Consequently, the electrostatic interaction between sepiolite particles and bacterial cells is not playing any significant role in explaining the antimicrobial effect of composite membranes.[47] Our data suggest that the antibacterial action of metal-loaded sepiolite membranes is only due to the release of soluble forms of silver and/or copper.

Metals have the potential to bind some proteins but not all biomolecules have a high level of discrimination and many can bind metal ions mimicking the correct cofactor.[48] When the metal homeostasis is affected the overproduction of ROS can induce oxidative stress resulting in cell damage.[49] Metal nanoparticles, attached to sepiolite, would then act as reservoirs for the release of metals that diffuse through the polymer towards the medium surrounding the membranes. Once in contact with living cells, the damage exerted by silver and copper ions proceed *via* several mechanisms associated or not with the production of reactive oxygen species (ROS). The following mechanisms have been identified as drivers explaining the antimicrobial activity of metals: (1) increased ROS production due to the *in vivo* induction of Fenton chemistry, the disruption of cellular donor ligands coordinating iron and thiol mediated reduction of metals; (2) protein dysfunction and loss of enzyme activity as a consequence of metal-catalysed oxidation of proteins in residues adjacent to metal-binding sites; (3) impaired membrane function due to metal binding on electronegative chemical groups; (4) interference with nutrient assimilation and (4) genotoxicity.[48,50–53] Noteworthy, the release of soluble metal ions from sepiolite fibers has been studied as the antibacterial way of action of natural silicates.[54]

The rate at which bacterial inactivation takes place has been studied during the first two hours after contact with membranes. Fig. 6 shows the results for membranes M(7), M(11) and M(12) loaded with SpAg, SpAgCu and SpCu respectively. In all cases, the membranes were inoculated with 10^6 cell per mL and incubated at 36 °C. Samples from the liquid culture in contact with them were taken at prescribed intervals during the first two hours, CFU counted and the results fitted to a first-order decay. The complete set of results for irradiated and non-irradiated membranes is presented in Table S1.† The antimicrobial effect was clearly faster in the membranes containing more silver, but it was also apparent for copper-loaded specimens. For SpAg@PSU–PVP-5, M(7) in Fig. 6, *E. coli* was completely inactivated in 60 min, while for SpCu@PSU–PVP-5, M(11), the decay was about 3 log (99.9%). Comparing successive uses of the same membrane, the rate of decay decreased, most probably due to the loss of the most external metal loading, after which silver and copper release slowed down.

The repeated reuse of membranes led to the results shown in Fig. 7 for M(7), M(11) and M(12) membranes, which were daily inoculated (10^6 cells per mL, 0.15 mL mg^{-1} of membrane), cultured for 24 h at 36 °C in 1/500 NB and, subsequently, washed, dried and reused in the same conditions. The number of daily reuses without appreciable microbial growth in plate count agar (<10 CFU mL^{-1} or 20 CFU cm^{-2}) was recorded as "days free of bacterial growth" (Fig. 7). It has to be taken into account that the number of cycles without significant bacterial count has been recorded under conditions very favourable to bacterial growth: at their optimal temperature and without any nutrient restriction. It is interesting to note that SpAg@PSU–PVP-5, M(7), displayed the better results against *E. coli* colonization but SpAgCu@PSU–PVP-5, M(11), which combines silver and copper, performed better against *S. aureus*. These data suggest a synergistic disinfection effect obtained by the combinations of both metals.

The number of cycles free of bacterial growth was generally higher for *S. aureus*. However, the rate of CFU decay for short time contacts (Table S1†) was lower for *S. aureus*. Gram-negative bacteria exhibit a thin layer of peptidoglycan between the cytoplasmic membrane and the outer cell wall whereas Gram-positive species possess a layer of peptidoglycan many times thicker.[55] This layer is known to help bacteria to overcome physical stresses and is also believed to reduce the penetration of toxic metal ions. Gram-negative bacteria possess an outer membrane with porins that can act as channels for low molecular weight substances to enter the cell.[56] Therefore, the tolerance to metal ions is generally higher for Gram-positive
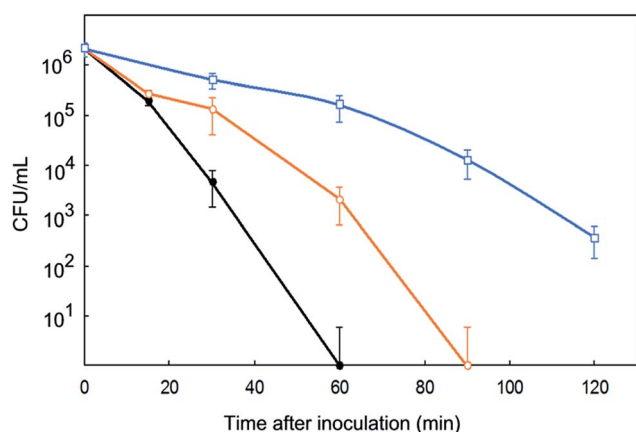

Fig. 6 Removal of *E. coli* in contact with M(7) (SpAg, ●), M(11) (SpAgCu, ○) and M(12) (SpCu, □) membranes during their first use.
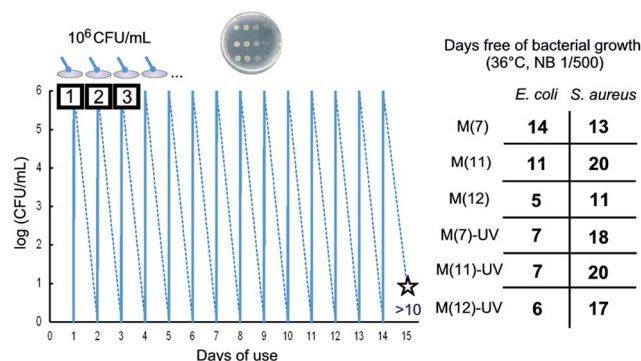

Fig. 7 Schematic view of successive daily inoculations until detecting bacterial colonies (the figure corresponds to M(11) incubated with *E. coli*) and days until detecting colonies of *E. coli* and *S. aureus*.

bacteria in agreement with the kinetic results obtained in this work (Table S1†). The fact that membranes were more efficient in the long term against *S. aureus* (Fig. 7) was not probably related to the vulnerability to silver or copper but to the higher growth rate of *E. coli*, which would overcome an intrinsically higher susceptibility.[57,58]

The data showed that metal release was the factor behind the antimicrobial behaviour of composite membranes. Therefore, the time on service of metal-doped membranes could be estimated from their initial metal content and the rate of metal release. From the data shown in Fig. 3, the time on service for metal loaded membranes could be roughly estimated in the order of 100 days (from copper release) or 300 days (calculated from silver release). The rate of metal release can be modulated using the amount of PVP. For example, for M(3), a membranes without PVP, it took 7 days to release >0.5% of the initial silver content (compared to 3 days for 1% in M(7) as shown in Fig. 3). The antimicrobial efficiency of membranes with lower metal release rate such as M(2) in Fig. 4 was considerably lower under the conditions tested in this work (36 °C, 1/500 NB), but under actual service conditions, at lower temperature and without a rich culture media, a material with lower rate of metal release could be competitive.

Conclusions

PSU–PVP membranes loaded with up to 5 wt% sepiolite containing silver and/or copper were produced. The introduction of PVP and UV-irradiation resulted in permeability increase and higher rate of metal release. Metal-loaded sepiolite became evenly dispersed within the membranes, without evidence of aggregates. Consistent with it, membrane surface charge, measured as ζ-potential, did not change significantly with the introduction of metal-loaded sepiolite. No nanoparticle leaching was detected.

The antibacterial performance of sepiolite-loaded membranes was high, with complete removal of bacterial colonies detached from membrane surface (<20 CFU cm^{-2}) and in the liquid culture in contact with them (<10 CFU mL^{-1}) for 5 wt% silver, copper or silver–copper sepiolite. SEM images showed membranes completely free of bacteria, compared to the high colonisation of PSU–PVP membranes.

The antimicrobial action was attributed to the release of metals diffusing from their supports. For membranes loaded with silver or silver–copper, the silver released daily amounted to 0.2–0.4% of the total silver content, which dropped one order of magnitude in the presence of chlorides in the medium. In contact with all metal-loaded composites, *E. coli* was quickly inactivated (<99.999% in 60 min for SpAg@PS–PVP-5). *S. aureus* inactivation was 5–10 times slower, which agrees with its Gram-positive nature.

Composite membranes containing silver and/or copper sepiolites could be successfully reused after daily inoculations and subsequent washing up to 20 times with <99.999% CFU removal. Despite of its initial lower rate of inactivation, the capacity to inactivate *S. aureus* lasted longer (an average of 8 cycles more) that to *E. coli*. Higher rates of metal release limited

membrane durability for the removal of *E. coli*, but not for *S. aureus*, indicating that the inactivation of the former requires higher concentrations of metals.

References

1 J. Schewe, J. Heinke, D. Gerten, I. Haddeland, N. W. Arnell, D. B. Clark, R. Dankers, S. Eisner, B. M. Fekete, F. J. Colón-González, S. N. Gosling, H. Kim, X. Liu, Y. Masaki, F. T. Portmann, Y. Satoh, T. Stacke, Q. Tang, Y. Wada, D. Wisser, T. Albrecht, K. Frieler, F. Piontek, L. Warszawski and P. Kabat, *Proc. Natl. Acad. Sci.*, 2014, **111**, 3245–3250.

2 M. M. Pendergast and E. M. Hoek, *Energy Environ. Sci.*, 2011, **4**, 1946–1971.

3 E. Filloux, B. Teychene, A. Tazi-Pain and J. P. Croue, *Sep. Purif. Technol.*, 2014, **134**, 178–186.

4 C. Fritzmann, J. Löwenberg, T. Wintgens and T. Melin, *Desalination*, 2007, **216**, 1–76.

5 T. Tweddle, O. Kutowy, W. Thayer and S. Sourirajan, *Ind. Eng. Chem. Prod. Res. Dev.*, 1983, **22**, 320–326.

6 T. Nguyen, F. A. Roddick and L. Fan, *Membranes*, 2012, **2**, 804–840.

7 W. Gao, H. Liang, J. Ma, M. Han, Z. Chen and Z. S. Han, *Desalination*, 2011, **272**, 1–8.

8 T. Nguyen, F. A. Roddick and L. Fan, *Membranes*, 2012, **2**, 804–840.

9 N. Park, B. Kwon, I. S. Kim and J. Cho, *J. Membr. Sci.*, 2005, **258**, 43–54.

10 Y. F. Zhao, L. P. Zhu, Z. Yi, B. K. Zhu and Y. Y. Xu, *J. Membr. Sci.*, 2013, **440**, 40–47.

11 Q. Sun, Y. Su, X. Ma, Y. Wang and Z. Jiang, *J. Membr. Sci.*, 2006, **285**, 299–305.

12 Y. Ma, F. Shi, J. Ma, M. Wu, J. Zhang and C. Gao, *Desalination*, 2011, **272**, 51–58.

13 B. Chakrabarty, A. Ghoshal and M. Purkait, *J. Membr. Sci.*, 2008, **315**, 36–47.

14 H. Matsuyama, T. Maki, M. Teramoto and K. Kobayashi, *Sep. Purif. Technol.*, 2003, **38**, 3449–3458.

15 M. J. Han and S. T. Nam, *J. Membr. Sci.*, 2002, **202**, 55–61.

16 Q. Li, S. Mahendra, D. Y. Lyon, L. Brunet, M. V. Liga, D. Li and P. J. Alvarez, *Water Res.*, 2008, **42**, 4591–4602.

17 J. A. Lemire, J. J. Harrison and R. J. Turner, *Nat. Rev. Microbiol.*, 2013, **11**, 371–384.

18 K. Zodrow, L. Brunet, S. Mahendra, D. Li, A. Zhang, Q. Li and P. J. Alvarez, *Water Res.*, 2009, **43**, 715–723.

19 A. Dasari, J. Quirós, B. Herrero, K. Boltes, E. García-Calvo and R. Rosal, *J. Membr. Sci.*, 2012, **405–406**, 134–140.

20 C. Beer, R. Foldbjerg, Y. Hayashi, D. S. Sutherland and H. Autrup, *Toxicol. Lett.*, 2012, **208**, 286–292.

21 Z. M. Xiu, Q. B. Zhang, H. L. Puppala, V. L. Colvin and P. J. Alvarez, *Nano Lett.*, 2012, **12**, 4271–4275.

22 K. D. Grieger, I. Linkov, S. F. Hansen and A. Baun, *Nanotoxicology*, 2012, **6**, 196–212.

23 J. Quirós, S. Gonzalo, B. Jalvo, K. Boltes, J. A. Perdigón-Melón and R. Rosal, *Sci. Total Environ.*, 2016, **563–564**, 912–920.

24 A. Esteban-Cubillo, R. Pina-Zapardiel, J. S. Moya, M. F. Barba and C. Pecharromán, *J. Eur. Ceram. Soc.*, 2008, **28**, 1763–1768.

25 A. Esteban-Cubillo, C. Pecharromán, E. Aguilar, J. Santarén and J. S. Moya, *J. Mater. Sci.*, 2006, **41**, 5208–5212.

26 L. Guo and P. H. Santschi, Ultrafiltration and its applications to sampling and characterisation of aquatic colloids, in *Environmental Colloids and Particles Behaviour, Separation and Characterisation*, IUPAC Series on Analytical and Physical Chemistry of Environmental Systems, ed. K. J. Wilkinson and J. R. Lead, John Wiley, Chichester, 2007, vol. 10, pp. 159–221.

27 P. Aerts, I. Genne, S. Kuypers, R. Leysen, I. F. J. Vankelecom and P. A. Jacobs, *J. Membr. Sci.*, 2000, **178**, 1–11.

28 P. Moradihamedani and A. H. B. Abdullah, *Desalin. Water Treat.*, 2016, **57**, 25542–25550.

29 H. T. Yeo, S. T. Lee and M. J. Han, *J. Chem. Eng. Jpn.*, 2000, **33**, 180–184.

30 M. Nyström and P. Järvinen, *J. Membr. Sci.*, 1991, **60**, 275–296.

31 K. S. Kim, K. H. Lee, K. Cho and C. E. Park, *J. Membr. Sci.*, 2002, **199**, 135–145.

32 G. Socrates, *Infrared and Raman characteristic group frequencies: tables and charts*, John Wiley & Sons, New York, 2004.

33 A. Rivaton and J. Gardette, *Polym. Degrad. Stab.*, 1999, **66**, 385–403.

34 X. Zhu, P. Lu, W. Chen and J. Dong, *Polymer*, 2010, **51**, 3054–3063.

35 M. A. S. Sadjadi, B. Sadeghi, M. Meskinfam, K. Zare and J. Azizian, *Phys. E*, 2008, **40**, 3183–3186.

36 L. M. Lyu, W. C. Wang and M. H. Huang, *Chem.–Eur. J.*, 2010, **16**, 14167–14174.

37 R. T. Downs and M. Hall-Wallace, *Am. Mineral.*, 2003, **88**, 247–250.

38 R. A. Festa and D. J. Thiele, *Curr. Biol.*, 2011, **21**, R877–R883.

39 J. Quirós, J. P. Borges, K. Boltes, I. Rodea-Palomares and R. Rosal, *J. Hazard. Mater.*, 2015, **299**, 298–305.

40 C. Jucker and M. M. Clark, *J. Membr. Sci.*, 1994, **97**, 37–52.

41 O. Habimana, A. J. C. Semião and E. Casey, *J. Membr. Sci.*, 2014, **454**, 82–96.

42 C. Carlson, S. M. Hussain, A. M. K. Schrand, L. Braydich-Stolle, K. L. Hess, R. L. Jones and J. J. Schlager, *J. Phys. Chem. B*, 2008, **112**, 13608–13619.

43 O. Choi and Z. Q. Hu, *Environ. Sci. Technol.*, 2008, **42**, 4583–4588.

44 G. Ren, D. Hu, E. W. Cheng, M. A. Vargas-Reus, P. Reip and R. P. Allaker, *Int. J. Antimicrob. Agents*, 2009, **33**, 587–590.

45 J. Ramyadevi, K. Jeyasubramanian, A. Marikani, G. Rajakumar and A. A. Rahuman, *Mater. Lett.*, 2012, **71**, 114–116.

46 X. Yang, A. P. Gondikas, S. M. Marinakos, M. Auffan, J. Liu, H. Hsu-Kim and J. N. Meyer, *Environ. Sci. Technol.*, 2011, **46**, 1119–1127.

47 V. Kochkodan and N. Hilal, *Desalination*, 2015, **356**, 187–207.

48 J. A. Lemire, J. J. Harrison and R. J. Turner, *Nat. Rev. Microbiol.*, 2013, **11**, 371–384.

49 P. P. Fu, Q. Xia, H. M. Hwang, P. C. Ray and H. Yu, *J. Food Drug Anal.*, 2014, **22**, 64–75.

50 Y. E. Lin, R. D. Vidic, J. E. Stout, C. A. Mccartney and V. L. Yu, *Water Res.*, 1998, **32**, 1997–2000.

51 J. Kim, H. Cho, S. Ryu and M. Choi, *Arch. Biochem. Biophys.*, 2000, **382**, 72–80.

52 J. P. Ruparelia, A. K. Chatterjee, S. P. Duttagupta and S. Mukherji, *Acta Biomater.*, 2008, **4**, 707–716.

53 Q. L. Feng, J. Wu, G. Q. Chen, F. Z. Cui, T. N. Kim and J. O. Kim, *J. Biomed. Mater. Res.*, 2000, **52**, 662–668.

54 C. C. Otto and S. E. Haydel, *PLoS One*, 2013, **8**, e64068.

55 T. J. Silhavy, D. Kahneand and S. Walke, *Cold Spring Harbor Perspect. Biol.*, 2010, **2**, a000414.

56 M. Yasuyuki, K. Kunihiro, S. Kurissery, N. Kanavillil, Y. Sato and Y. Kikuchi, *Biofouling*, 2010, **26**, 851–858.

57 H. Yamada, N. Takahashi, S. Okuda, Y. Tsuchiya and H. Morisaki, *Appl. Environ. Microbiol.*, 2010, **76**, 5409–5414.

58 S. Heß and C. Gallert, *Microb. Ecol.*, 2016, **72**, 1–11.